



# Higgs Bosons in the Dijet Spectrum of Black Hole Decays at CMS

N. Akchurin<sup>a</sup>, J. Damgov<sup>b</sup>, D. Green<sup>b</sup>, S. Kunori<sup>c</sup>, G. Landsberg<sup>d</sup>, J. Marraffino<sup>b</sup>, R. Vidal<sup>b</sup>, H. Wenzel<sup>b</sup>, W. Wu<sup>b\*</sup>

<sup>a</sup>*Texas Tech University, Lubbock, Texas, U.S.A.*

<sup>b</sup>*Fermi National Acceleration Laboratory, Batavia, Illinois, U.S.A.*

<sup>c</sup>*University of Maryland, College Park, Maryland, U.S.A.*

<sup>d</sup>*Brown University, Providence, Rhode Island, U.S.A*

## Abstract

An intermediate-mass Higgs boson ( $m_H \sim 130 \text{ GeV}/c^2$ ) is one of most exciting examples of an undiscovered particle that can be produced by rapidly evaporating Black Holes at the LHC. If the energy scale of quantum gravity is near one TeV, the LHC will produce a Black Hole (BH) about once every second. Moreover, most BH decays contain at least one prompt, energetic photon or charged lepton, corresponding to final states with relatively low Standard Model backgrounds. About 6.6% of the BH decays will contain an intermediate-mass Higgs boson, producing a large sample of Higgs bosons at the LHC even at low luminosities. We have developed specific algorithms that yield a ratio of Higgs signal to background of approximately one when applied to the full CMS detector simulation and data reconstruction of BH Monte Carlo events. Because of the large number of Higgs bosons coming from BH production and decay, the significance of the signal will increase very quickly at the LHC. For only 46 thousand BH events, we found  $S/\sqrt{B}$  to be larger than 6. To produce 46 thousand BH events requires an integrated luminosity of about  $3 \text{ pb}^{-1}$ , or only a few hours of LHC operation at the nominal luminosity, if the fundamental Planck scale is as low as 2 TeV.

---

\*) send comments/questions to [weimin@fnal.gov](mailto:weimin@fnal.gov)

# 1 Introduction

An exciting consequence of TeV-scale quantum gravity in models with large spatial extra dimensions [1] is the possibility of production of Black Holes at CERN’s Large Hadron Collider (LHC) and other future colliders. As was shown recently [2, 3], the cross section for Black Hole (BH) production at the LHC is expected to be  $\sim 100$  pb for a fundamental Planck scale  $M_p \sim 1$  TeV, which would turn the LHC into a BH factory with a production rate of  $\sim 1$  Hz. BH’s with masses about 1 TeV quickly evaporate via Hawking radiation [5] into about a half dozen particles [2, 3]. The Hawking temperature of TeV-mass BH’s is a few hundred GeV, which allows the production of new particles with masses around  $100 \text{ GeV}/c^2$  in BH decays, specifically an intermediate-mass Higgs boson.

In a previous work [4], a Monte Carlo simulation study that used a parameterized detector reported the possibility of discovering new physics in the decays of BH’s. This previous study assumed a hadron calorimeter energy resolution of  $60\% / \sqrt{E}$ , and jets were reconstructed using a parton-level clustering algorithm. The significance of the Higgs signal was 6.7, for an integrated luminosity of  $\sim 3 \text{ pb}^{-1}$ .

Inspired by these results, we report a similar search for the Higgs boson in BH decays using a full simulation of the CMS detector at the LHC. In addition, by optimizing the selection criteria and algorithms, we were able to improve further the significance of the Higgs signal, despite the more realistic detector simulation and inclusion of overlapping minimum bias events expected at LHC luminosities.

## 2 Higgs Boson Production from the Decay of Black Holes

It is expected that BH production turns on rapidly once the relevant energy threshold ( $\sim M_p$ ) is crossed [2, 3]. At lower energies, we expect BH production to be exponentially suppressed due to the string excitation or other quantum effects. At the LHC, the total production cross section for a Black Hole with mass  $> M_p$  typically varies between about 1 pb and 15 nb (for a Planck scale between 1 TeV and 5 TeV) and can vary by  $\sim 10\%$  depending on  $n$ , the number of large extra dimensions (between 2 and 7). For Monte Carlo events in this study, the Planck scale was set to 1.0 TeV, and we assumed there were only 3 extra dimensions, resulting in a large BH production cross section of 15 nb at the LHC.

The decay of a BH is governed by its Hawking temperature, which is inversely proportional to its Schwarzschild radius. As the parton collision energy increases, the resulting BH’s get heavier and their decay production gets colder. Also, note that the wavelength  $\lambda$  corresponding to the Hawking temperature is larger than the size of the BH. Therefore, to first approximation, the BH is a point-radiator and emits mostly S-waves [6]. Since it is only sensitive to the radial coordinate and does not make use of the extra angular modes available in the bulk, it decays equally into particles on the brane and in the bulk. Since there are many more particles on our brane than in the bulk, this has the crucial consequence that the black hole decays mostly to the familiar Standard Model particles [6].

The average number of Standard Model particles produced in a BH evaporation at the LHC energies for the fundamental Planck scale of 2 TeV and 3 extra dimensions is about 5. After these parent particles decay, the average multiplicity stays approximately constant event to event. Since a BH decays almost democratically, the typical decay emits all known Standard Model degrees of freedom roughly equally. A relatively large fraction of prompt and energetic photons, electrons, and muons are expected in these relatively high-multiplicity BH decays, which makes it possible to select a pure sample of BH events [2, 3]. It also makes it relatively easy to trigger on these events.

We are interested in the production of a Standard Model-like Higgs boson with an intermediate mass (130 – 150  $\text{GeV}/c^2$ ), predicted in a variety of low-scale supersymmetry and Technicolor models. We consider only decays of the Higgs boson into a jet pair, dominated by the  $b\bar{b}$  final state ( $\sim 50\%$ ), with additional  $\sim 10\%$  contribution from the  $c\bar{c}$ ,  $g\bar{g}$ , and hadronic  $\tau\tau$  final states. The decay of a BH is thermal; it obeys all local conservation laws, but otherwise does not discriminate between particle species (that is, particles with approximately the same mass and spin). Since there are six charged leptons and one photon, we expect  $\sim 10\%$  of the particles to be hard, primary leptons and  $\sim 2\%$  of the particles to be hard photons, each with hundreds of GeV of energy. This is a clean signal with negligible background since the production of Standard Model leptons or photons in high-multiplicity events at the LHC occurs at a much smaller rate than in BH production. These events are also relatively easy to trigger on, since they contain at least one prompt lepton or photon with energy above 100 GeV, in addition to energetic jets. Furthermore, since there are just three neutrinos, we expect only  $\sim 5\%$  average missing transverse energy ( $\cancel{E}_T$ ) per event, which allows us to estimate the BH mass from the visible decay products with precision.

### 3 Event Generation

We simulate black hole production and decay at the LHC using TRUENOIR [8] Monte Carlo code interfaced with PYTHIA [9] event generator. Technically, the code generates black holes in  $p\bar{p}$ , and not  $pp$  collisions, but at the high energy offered by the LHC this difference is not important. MRSD-' parton distribution functions [10] are used to provide an adequate description of black hole formation. It is assumed that the evaporation of black hole happens suddenly, at its formation Hawking temperature. This is a reasonable assumption, since an evaporating black hole spends most of its time near its original temperature, as the Hawking radiation spectrum is softest at this temperature, and becomes harder and harder as the temperature rapidly increases in the process of evaporation [2].

As mentioned above, once produced, the black hole evaporates in approximately half-a-dozen particles, each carrying hundreds of GeV of energy. Electric charge, color charge, lepton and baryon numbers are all conserved in the evaporation process in our model. The probabilities of emission of various types of particles are estimated by counting the number of degrees-of-freedom (d.o.f.) for each individual particle, including all its quantum numbers. The whole host of the Standard Model particles and antiparticles corresponds to  $\approx 120$  d.o.f. Consequently, a light Higgs boson, which has a single d.o.f., should be emitted with  $\sim 1\%$  probability, while some 70% of the emitted particles are quark and gluons.

The generation is done for a fixed case of  $n = 3$  extra dimensions and the fundamental Planck Scale of 2 TeV. Generated events are dumped in the HEPEVT format in an binary file for further processing via standard CMS detector response simulation packages. The total cross section of black hole production for this set of parameters is 450 pb. A total of 50K and 100K events have been generated at two Higgs masses of 130 and 150 GeV.

### 4 CMS OSCAR Simulation and ORCA Production

A detailed description of the CMS detector can be found in Refs. [7, 11, 12]. The distinctive features of the CMS detector are the following: a 4 Tesla axial magnetic field, a multi-layer muon system in the return yoke, a scintillating crystal electromagnetic calorimeter (ECAL), a sampling hadron calorimeter (HCAL), and an all-silicon inner tracking system based on fine-grained micro-strip and pixel detectors. The calorimeter and the tracker are located inside the solenoid in the magnetic field. The sampling hadron calorimeter extends up to pseudo-rapidity  $|\eta| = 5$ , and consists of 4 mm thick plastic scintillator tiles inserted between brass absorber plates. The barrel and endcap sections of the calorimeter are placed inside the solenoid. To measure the late shower development, an outer hadron calorimeter is located in the central region of the detector ( $|\eta| < 1.3054$ ), outside the solenoid in the barrel return yoke. The lateral granularity of the calorimeter towers is  $\delta\eta \times \delta\phi = 0.087 \times 0.087$  for  $|\eta| < 2$ . The calorimeter readout has a dynamic range from 200 MeV to 3 TeV, to allow single muons to be observed [7] as well as very energetic jets. Test beam studies with a full ECAL plus HCAL prototype indicate that an energy resolution of  $112\%/\sqrt{E} \oplus 3.6\%$  (E in GeV) is achievable for single pions with energies between 20 GeV and 300 GeV [11]. To extend the hermeticity of the hadron calorimeter up to  $|\eta| = 5.31$ , a separate forward calorimeter is placed at a distance of 11 meters from the interaction point along each beam-line. Because this calorimeter is located in a high radiation and high rate environment, it uses quartz fibers as an active medium, embedded in the iron absorber wedges [12], and is read-out using high-gain phototubes.

For this study, the detector is assumed to be accurately calibrated and aligned. For the pixel and silicon strip detectors, an alignment with an accuracy of about  $10\mu m$  in all three dimensions is required. To simulate the detector, a GEANT4-based detector simulation package called OSCAR (version 2.4.6) [13], was used. The output from the OSCAR simulation is the deposited energy in the sensitive volumes. After simulation, the events are processed with a CMS detector reconstruction program called ORCA (version 7.6.1, Object-oriented Reconstruction for CMS Analysis) [14]. The detailed and complete process of signal formation is included in the first stage of ORCA. For example, for HCAL, this includes the photo-statistics, QIE pulse shape, ADC quantization, and electronics noise. At this point, the data for an event is saved as a persistent object in a Objectivity federation database. This digitized data is read by ORCA in the second stage to form the higher level objects (jets, tracks etc). Using the CMS JetMET analysis code in ORCA, the higher level objects are then stored in a ROOT files making it convenient for fast interactive analysis and batch processing.

Jets are reconstructed by using an iterative cone algorithm with cone size 0.5 in  $(\eta, \phi)$  space. Input for this algorithm are "trigger towers" with  $E_T > 0.5$  GeV. A trigger tower is formed by summing an HCAL tower and the

corresponding ECAL 5 x 5 crystal matrix directly in front of the tower. The ROOT file also contains all available information at the Monte Carlo generator level concerning the particle kinematics, vertexes, missing transverse energy, etc.

## 5 Kinematics of Black Hole Events at the LHC

BH events at the LHC have unique and unusual kinematics compared to the more familiar Standard Model events. The total energy and total transverse energy (*i.e.* scalar sum- $E_T$ ) in BH events is unusually large (Figures 1 & 2), with a mean value of 2.9 TeV and 1.8 TeV respectively. For the 46K BH events simulated, there were 6.6 K Z's, 13.6 K top-quarks, 3.1 K Higgs bosons, 19.8 K W's, and a number of gluons, photons, quarks and leptons found in the events, showing the democratic nature of the BH decays. The jet multiplicity is large with a mean value above 4 for jets with  $E_T > 50$  GeV (Figure 3). There is a large number of charged leptons (electrons and muons) with large  $E_T$ , making them easy to distinguish from leptons from the usual Standard Model processes (Figure 4). In our previous physics studies for single t-quarks,  $t\bar{t}H$ ,  $qqH$  [7, 15, 16] etc. (with backgrounds like  $t\bar{t}$ ,  $t\bar{t}$ +jets, W+jets, etc.) the  $E_T$  distribution of the highest  $E_T$  lepton usually peaked at less than 50 GeV. Such large  $E_T$  primary leptons in BH events makes triggering simple and efficient, and can be used to remove most Standard Model backgrounds. Therefore, in this study, we chose not to include these backgrounds and to concentrate on the BH events exclusively since the di-jet background is dominated by the combinatorics from BH events themselves.

Unlike the Standard Model processes that produce Higgs bosons at the LHC (gluon and W-boson fusion [7]), BH events often contain multiple jets, leptons and bosons (like W's, Z's, b-quarks, and t-quarks) produced in association with the Higgs boson. There is even a small probability that the BH events actually contain more than one Higgs boson ( $\sim 1\%$ ). When these extras heavy particles decay, they create additional combinatoric problems when trying to identify Higgs bosons in BH events. Also, their decays can produce neutrinos in the event and this could in principle increase the missing transverse momentum. Fortunately, this is not the case since the additional neutrinos are not very correlated and the missing transverse momentum is not significantly larger than that for the average Standard Model events (Figure 5). The mean value of the mass of the black hole in the generated sample was 3.1 TeV (Figure 6). The number of final state objects defined as jets ( $E_T > 25$  GeV) plus leptons ( $E_T > 50$  GeV) has a mean value of 5.6.

While the rapidity distribution of Higgs bosons produced in BH events is similar to that in Standard Model production, the momentum distribution is very much harder. The mean value of the  $E_T$  for Higgs bosons in BH events is approximately 450 GeV (Figure 7). Such large momentum Higgs bosons have two major effects on the identification and analysis. For  $\bar{b}b$  decays of the Higgs boson, the opening angle between the two b-jets is quite small, making the usual jet-finding algorithms inefficient unless the algorithms are capable of handling merged jets. However, in the case of BH production, even for low luminosities, the number of Higgs bosons produced at the LHC is large enough that we can afford significant inefficiencies in the jet finding and still obtain a substantial Higgs sample. More serious is the problem of b-tagging such energetic jets using the silicon tracking of CMS. The transverse energy of b-jets from Higgs boson in BH events is quite high (Figure 8). The b-tagging efficiency decreases rapidly for jets exceeding 100 GeV as they become more collimated, the individual tracks more difficult to distinguish, and the displaced b-vertex harder to identify. Figure 9 shows the transverse energy of the final jets for all di-jet combinations after the analysis cuts. There is a long and substantial tail extending to large  $E_T$ . Current b-tagging algorithms may have to be improved to increase the tagging efficiency if a larger sample of Higgs bosons is needed.

## 6 Strategy and Development of Physics Analysis

The CMS hadron calorimeter (HCAL) was designed to have a resolution of about  $120\%/\sqrt{E} \oplus 4\%$  for single pions. Consequently, for a jet energy of 20 GeV, the jet resolution is about 26.8%; about 16.9% for a jet energy of 50 GeV; and 12% for 100 GeV. The standard CMS reconstruction and analysis code (ORCA, version 7.6.1) contains jet reconstruction that uses only the calorimeter information. There has been considerable effort in CMS to improve the jet energy resolution by including momentum information from charged tracks [17]. In these studies, the jet energy resolution was improved to 13%, 10% and 8% compared to 26.8, 16.9, and 12%, for jet

energies 20, 50, 100 GeV respectively. However, this “advanced-jet package”, which combines calorimeter and track information, was tested only for jet energies up to about 120 GeV, and only for Standard Model QCD di-jet production. Since the jet energies are much larger in BH decays, we do not expect at this time (and without further study) any significant improvement in the jet energy resolution (beyond the calorimeter-only jet reconstruction) for the jets coming from Higgs bosons in BH decays. Therefore, we used only the standard jet reconstruction in ORCA, which should be sufficient for this initial study.

Since the jets coming from Higgs bosons in BH decays are very energetic, we can safely select only jets with  $E_T$  greater 50 GeV (compared to the usual 25 GeV in typical CMS analysis) without losing a significant signal efficiency. A larger jet  $E_T$  cut also reduces the jet-pair combinatorics, suppresses the number of jets coming from other interactions in the same beam crossing, and improves slightly the jet energy resolution, improving the di-jet mass resolution. (The jet  $E_t$  resolution at 50 GeV is about 21.1% compared with 25.1% for 25 GeV).

As mentioned before, to reduce the Standard Model backgrounds, we also require that there be at least one charged muon or electron in the event with  $E_T > 50$  GeV. However, requiring two 50 GeV jets and a 50 GeV charged lepton is not enough to separate the Higgs boson signal from all backgrounds. Figure 10 shows the di-jet mass using a clustering algorithm for particles produced by the BH Monte Carlo generator before reconstruction in the CMS detector (generator level). A clear peak is visible above background at the Higgs boson mass. However, after simulation and reconstruction in the CMS detector, Figure 11 shows the same di-jet mass distribution. The peak at the Higgs mass is not very obvious. Clearly, further requirements are needed to improve the signal to background for the Higgs boson. Therefore, we examined various strategies:

- Since the Higgs is a scalar boson, if we plot the cosine of the angle ( $\theta^*$ ) between the direction of the Higgs boson (the parent) and one of its decay products (the  $b$  jet), in the Higgs rest frame, the distribution should be isotropic. In contrast, for most other di-jet mass combinations (e.g. from QCD), the distribution is peaked toward the forward direction due to the dominance of the t-channel exchange (Figure 12). If we require  $|\cos \theta^*| < 0.8$ , we will preferentially remove background combinations.
- Selecting on the correlations in the angular distributions of the jets, or jet pairs, is the obvious candidate for further development. In many two-jet mass analysis for Standard Model physics, a requirement is often placed on the parton scattering angle to reduce the contamination from QCD two-jet scattering, since there is a large QCD contribution from the t-channel. Although we have not included any Standard Model backgrounds, this requirement also is useful in eliminating many of the wrong two-jet combinations in BH events, since Higgs bosons in BH decays are highly boosted and the opening angle between the two jets is small. We can assign the scattering angle ( $\hat{\theta}$ ) for the parton subprocess (measured relative to the initial parton direction) to be the beam direction at the LHC. Then, from kinematics:

$$\cos \hat{\theta} = \tanh \hat{\eta} = \tanh \frac{\eta_1 - \eta_2}{2} \quad (1)$$

For the Higgs boson in BH decays, there should be a peak at zero (Figure 13) while in general, uncorrelated di-jets should be uniform (Figure 14). From the Figures 13 and 14, requiring  $|\cos \hat{\theta}|$  to be less than 0.2, will keep most of the Higgs signal and remove a large fraction of the background. This is a more stringent requirement than usual. It is only possible because of the large momentum of the Higgs boson in BH events.

- Furthermore, since a Higgs boson in BH decays has large momentum, the opening angle between the jets in the decay of the Higgs is small, and thus their separation in  $\eta - \phi$  space is also small (Figures 15 & 16). The standard jet-finding algorithm in CMS’s ORCA uses a cone size of 0.5 in  $\eta - \phi$  space, and is somewhat inefficient for these Higgs boson decays because it often finds a single jet rather than the two jets in the decay. Moreover, if the two jets overlap in  $\eta - \phi$  space, but are still found as separate jets, the algorithm often assigns some energy to the wrong jet, degrading the di-jet mass resolution. However, after much explication, surprisingly, we found that the best strategy for identifying the Higgs decays and reducing the background is to require that the two jets be separated by less than 1.0 in  $\eta - \phi$  space for the standard cone algorithm of 0.5. This requirement lowers the efficiency for the Higgs signal, but is simple and straightforward compared with developing a new efficient jet-finding algorithm to deal with overlapping jets. Since the production rate for Higgs bosons from BH events is quite large, the loss of efficiency following this strategy is not prohibitive, and the background rejection is significant.

## 7 Analysis and Results

### 7.1 Analysis

The analysis used the information contained in a ROOT file constructed from the output of the CMS's ORCA reconstruction program. The analysis followed six steps and is summarized below:

- To simplify and expedite the analysis, we used only leptons and photons identified by the Monte Carlo generator rather than the current lepton and photon identification algorithms in CMS's ORCA. For electrons, muons, and photons, we defined isolation such that there are no nearby jets found within a cone of radius 0.5 in  $\eta - \phi$  space centered on the lepton or photon. We required  $E_T > 50$  GeV and  $|\eta| < 2.5$  for each lepton or photon. We required a least one such isolated lepton or photon in the event. These requirements eliminate most of the Standard Model backgrounds as we have mentioned previously, and satisfy the expected trigger conditions for BH events in CMS. The final number of events should be multiplied by the actual (experimentally determined) identification efficiencies for leptons and photons, as well as the CMS trigger efficiency.
- Since  $\sim 50\%$  of the Higgs bosons with mass 130 GeV decay to  $b\bar{b}$ , we concentrate on these decays exclusively. However, since the expected b-tagging efficiency in CMS is not large, we will require only one of the jets to come from a b-quark. This will help reduce the combinatorics and reduce the W/Z peak from the BH decays. Since the CMS b-tagging of jets is still under development (and needs to be developed even further for the large momenta in BH events), we applied a simple-minded b-tagging using the Monte Carlo generator level information as follows: for every b-quark generated, we calculate the distance ( $\delta R$ ) between the b-quark and each hadronic jet in  $\eta - \phi$  space; if  $\delta R$  for a jet is less than 0.7, then we mark the jet as b-tagged. We require there be at least one jet marked as b-tagged in the event, and require that at least one jet be marked b-tagged when making di-jet pairs. Our simplified b-tagging method assumes an ideal b-tagging efficiency (100 %) and a zero mis-tagging rate. With realistic b-tagging in the experiment, the signal significance could be degraded. This will be discussed later.
- For each di-jet combination in an event, we require that the scattering angle be consistent with BH production. We calculate the cosine of the scattering angle using (1) which relates the scattering angle to the  $\eta$ 's of the two jets as measured in the CMS detector. We require the absolute value be less than 0.2 (Figure 13). This suppresses the combinatoric "background" while keeping most of the di-jet combinations from the Higgs decays.
- Because the momentum of the Higgs boson is quite large, and thus the opening angle of the two jets from the Higgs decay, quite small, we require that the distance between the two jets in  $\eta - \phi$  space be less than 1.0, but larger than 0.6. This last requirement helps to avoid assigning calorimeter energy to the wrong jet, and degrading the di-jet mass resolution.
- Finally, we form all two-jet combinations in each event that satisfy the above criteria. We then calculate the di-jet invariant mass assuming zero mass for each jet and using the jet-cluster centroid as the b-quark direction. Figure 17 shows the di-jet invariant mass spectrum for the 46K BH events we simulated and analyzed. Compared to Figure 11, we can see a clear peak in Figure 17 in the Higgs mass region after our further selection requirements. Note also that the jet energies were corrected for the  $\eta$  variation of the calorimeters, and the energy scale was calibrated to reproduce the initial parton energies.

There are other selection criteria that one might consider applying to the data to improve the signal to background for the Higgs boson in BH events. Among others, we tried making a cut on the decay angle of the jets in the Higgs (di-jet) rest frame, raising the lepton/photon  $E_T$  requirement, making a cut on the scalar sum of the transverse energies of all calorimetry towers, cutting on missing transverse energy, or cutting on the number of jets and leptons. Most of these additional requirements (some of which are not independent from the criteria described above) had only a small effect on the signal to background for the Higgs boson. We chose to forgo adding any more additional requirements at this time until we have confirmed and perfected the above selection criteria with real data.

## 7.2 Results for $M_H = 130 \text{ GeV}/c^2$

From the di-jet invariant mass spectrum in Figure 17, we tried to estimate quantitatively the amount of Higgs signal and background. We first tried a maximum-likelihood fit to the di-jet spectrum using two Gaussian functions plus a quartic polynomial. (The two Gaussian functions correspond to the W/Z and the Higgs signals respectively, while the polynomial corresponds to the “combinatorial” background, as suggested in [4]. There are eleven parameters in the fit.) For comparison, we first try fitting the di-jet spectrum using only the particle clustering at the generator level. Figure 18 shows the result of the fit. In Figure 18, and the following Figures 19, 20, 22 and 25, the dash line represents a quartic polynomial curve, and the dotted line represents a Gaussian curves, and the solid line is the total spectrum as described above. A clear Higgs signal above the background around the Higgs mass region is evident as expected. Next, we apply the same fitting procedure to the reconstructed di-jet spectrum before the additional selection criteria. Figure 19 shows the result of the fit. Finally, we fit the di-jet mass spectrum after all the selection requirements (Figure 20).

In this fitting procedure, we have allowed the coefficients in the polynomial for the background to vary unconstrained. Since the Higgs signal events can effect the shape of the fitted background, this is perhaps not the best procedure to follow. We can get a more accurate estimate for the backgrounds by removing BH events that contain a Higgs boson, since they can be identified from the Monte Carlo generator information. We then fit the di-jet spectrum to a single Gaussian function (W/Z) and a quadratic polynomial, giving us a more accurate estimate of the real shape of the background. We then use the parameters of the quadratic polynomial to fit the full di-jet spectrum including the Higgs boson decays, allowing only the normalization of the polynomial to vary. (We also tried including the Higgs events and eliminating only the two-jet combinations that came from the Higgs decays, but the difference in shape was negligible. Therefore, we chose the simplest procedure, eliminating events with a Higgs boson decay entirely.)

Figure 21 shows the di-jet mass spectrum and fit for BH events with no Higgs boson produced. For comparison, Figure 22 shows the spectrum and fit for BH events that contain at least one Higgs boson. Figure 23 shows the spectrum and fit for all events, constraining the shape of the background as determined previously. If we add up the events within one standard deviation around the mean of the Higgs Gaussian, then we find 80 events for the Higgs and 94 background events. The signal significance is then  $S/\sqrt{B} = 8.2$ .

It is possible that b-tagging in CMS will not be fully functional at the very beginning of LHC running. Some time will be needed initially to test and develop the b-tagging algorithms for CMS, as well push their upper range to larger  $E_T$  jets. Since BH production at the LHC is so large, it may be possible to find evidence for a Higgs signal in the CMS detector without using b-tagging in the early stages of running. Figure 24 shows the di-jet mass spectrum for BH events without a Higgs boson produced in the decay where we have dropped the b-tag requirement. As expected, the W/Z peak is much larger relative to the background than in Figure 21, which required one jet to be b-tagged. If we follow the same procedure as previously and extract the background shape from Figure 24, fit the di-jet mass spectrum for all BH events, and integrate the di-jet mass spectrum around the Higgs peak, we find 114 Higgs and a background of 237 events. This gives a signal significance  $S/\sqrt{B} = 7.4$ , slightly worse than requiring at least one b-tagged jet. This result is similar to the previous study [4] which used a parameterized detector simulation with excellent energy resolution. The additional selection criteria that we developed here compensated for the more realistic detector simulation.

## 7.3 Results for $M_H = 150 \text{ GeV}/c^2$

We also explored another value for the Higgs mass ( $150 \text{ GeV}/c^2$ ). For this larger mass value, we expect the Higgs peak in the di-jet mass spectrum to be well separated from the W/Z. However, for a Higgs boson mass greater than  $135 \text{ GeV}/c^2$ , the dominant branching ratio is no longer  $b\bar{b}$ , since the Higgs boson prefers to decay more into  $W+W-$  instead (one of the W's is virtual). For a Higgs boson with mass  $150 \text{ GeV}/c^2$ , the branching ratio to  $b\bar{b}$  is only  $\sim 17\%$ , reduced by nearly a third. Furthermore, since the Higgs boson decays more often to  $W+W-$ , the jets from this decay add to the combinatorial background. Figure 24 shows the di-jet mass spectrum and fit at the generator level for BH events for  $M_H = 150 \text{ GeV}/c^2$ , which can be compared with Figure 18 where  $M_H = 130 \text{ GeV}/c^2$ .

We generated and processed 97K BH events where  $M_H = 150 \text{ GeV}/c^2$ . Obviously, the BH production cross section and decay into Higgs bosons is little changed for this larger mass. To produce 97K events BH events

requires an integrated luminosity of  $\sim 18.6 \text{ pb}^{-1}$ . We performed the same calculations and analysis as in the case where  $M_H = 130 \text{ GeV}/c^2$  to extract the signal significance, with and without b-tagging. The results were very similar. In summary, an integrated luminosity  $141 \text{ pb}^{-1}$  would be required in order to get the same signal significance as the case where  $M_H = 130 \text{ GeV}/c^2$ . (For  $M_H = 130 \text{ GeV}/c^2$ , an integrated luminosity of  $3 \text{ pb}^{-1}$  is required to get  $S/\sqrt{B} = 8.2$ .) This is a bit longer LHC running, but still represents only a few days at nominal luminosity.

## 8 Conclusions

The main discovery channels for the Higgs boson searches in CMS at LHC are summarized in Ref. [7]. There is also an alternative search for the Higgs in a more exotic mode involving low-scale gravity, Black Hole decay. In previous pioneering study [4], some promising results were obtained. Using a more realistic CMS detector simulation, we have developed specific algorithms that allowed us to improve the signal significance further. With as little as few days of operation of the LHC, we should be able to observe easily an intermediate-mass Higgs boson from the decay of Black Holes if TeV-scale quantum gravity exists.

## 9 Acknowledgments

We would like to thank Chris Tully for his useful discussion on the issue of HCAL resolution for various versions of ORCA and other important comments.



## References

- [1] N. Arkani-Hamed, S. Dimopoulos, and G. Dvali, Phys. Lett. B **429**, 263 (1998); I. Antoniadis, N. Arkani-Hamed, S. Dimopoulos, and G. Dvali, Phys. Lett. B **436**, 257 (1998); N. Arkani-Hamed, S. Dimopoulos, and G. Dvali, Phys. Rev. D **59**, 086004 (1999).
- [2] S. Dimopoulos and G. Landsberg, Phys. Rev. Lett. **87**, 161602 (2001).
- [3] S.B. Giddings and S. Thomas, Phys. Rev. D **65**, 056010 (2002).
- [4] G. Landsberg, Phys. Rev. Lett. **88**, 181801 (2002).
- [5] S.W.Hawking, Commum. Math. Phys. **43**, 199 (1975).
- [6] R. Emparan, G.T. Horowitz and R.C. Myers, Phys. Rev. Lett. **85**, 499 (2000).
- [7] Summary of the CMS potential for the Higgs Boson Discovery 10 Dec. 2003, CMS Note 2003/033.
- [8] S. Dimopoulos and G. Landsberg, preprint SNOWMASS-2001-P321, June 2001, published in eConf **C010630**, P321 (2001).
- [9] T. Sjöstrand, L. Lönnblad, and S. Mrenna, e-print hep-ph/0108264. We used v6.157.
- [10] A.D. Martin, R.G. Roberts, and W.J. Stirling, preprint RAL-92-078 (1992).
- [11] CMS collaboration, Technical Design Report(TDR), CERN/LHCC 2000-016, Feb. 2000.
- [12] CMS collaboration, The Hadron Calorimeter Project, Technical Design Report(TDR), CERN/LHCC 97-31.
- [13] CMS collaboration, CMS Simulation and Reconstruction Package <http://cmsdoc.cern.ch/OSCAR/>.
- [14] <http://cmsdoc.cern.ch/orca/>.
- [15] D. Green et al., A study of  $t\bar{t} + H$  at CMS, CMS note 2001-039.
- [16] N.Akchurin et al., Search for the SM Higgs using  $pp \rightarrow q\bar{q} H$  at CMS, CMS note 2002-016.
- [17] S. Abudullin et al., CMS IN-2001/037.

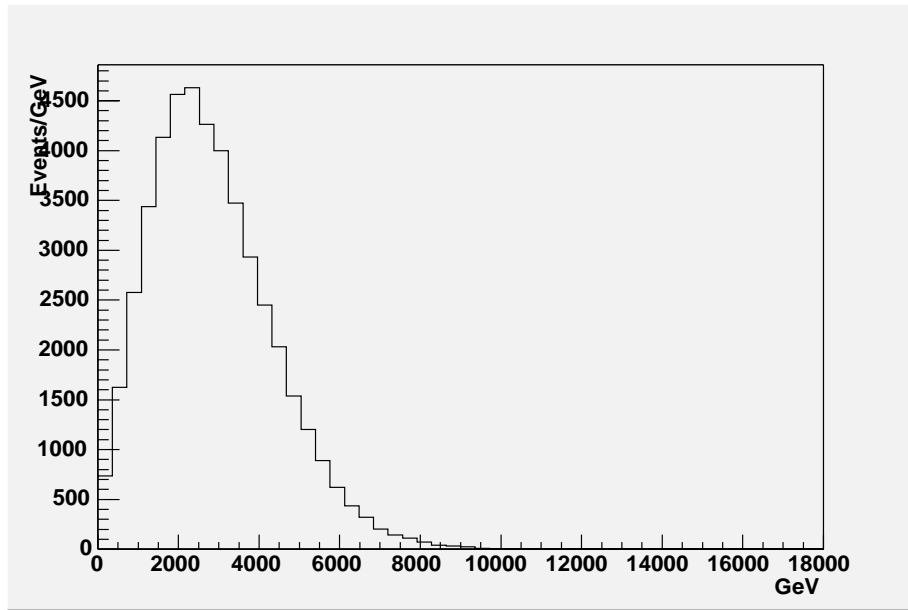


Figure 1: Total energy in BH events

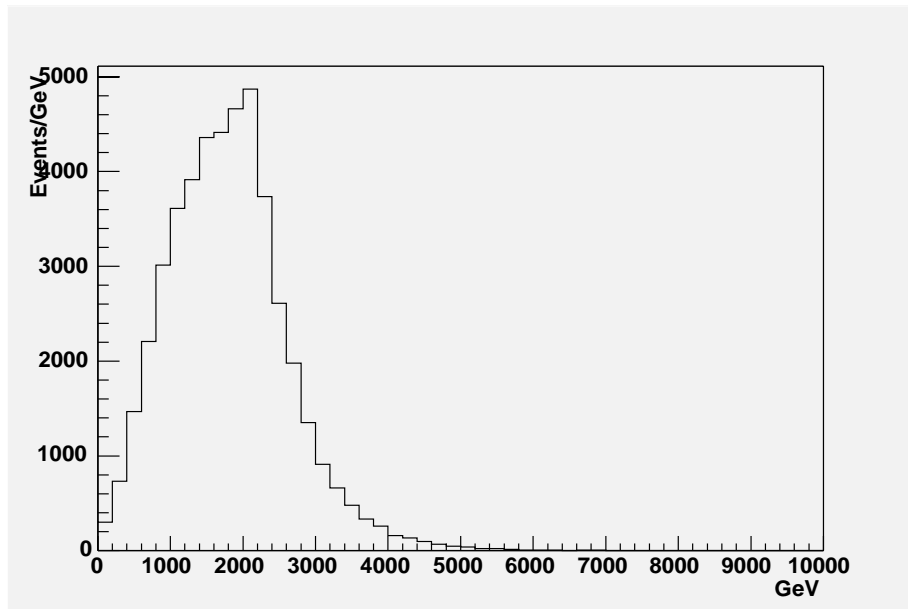


Figure 2: Total transverse energy (scalar)sum-Et in BH events

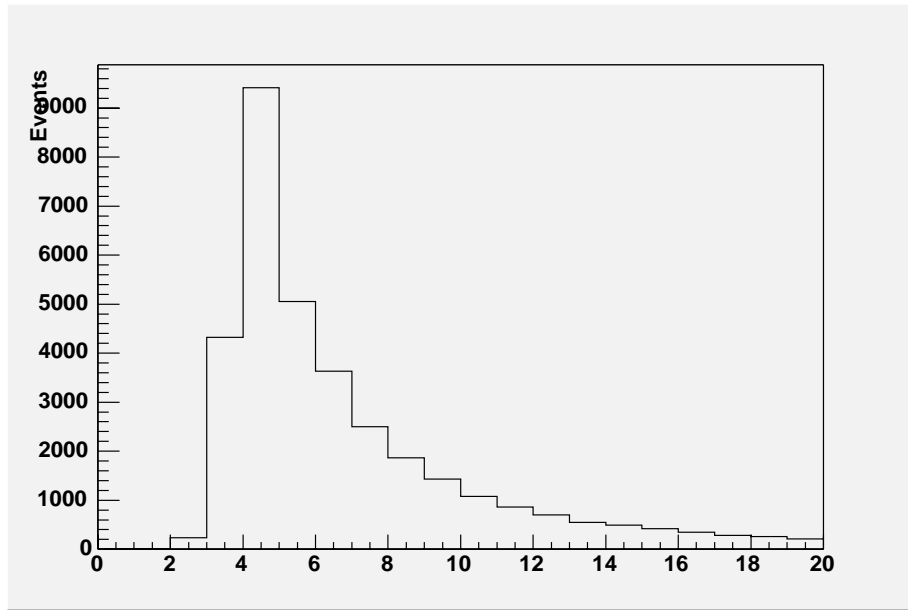


Figure 3: Jet multiplicity for BH events

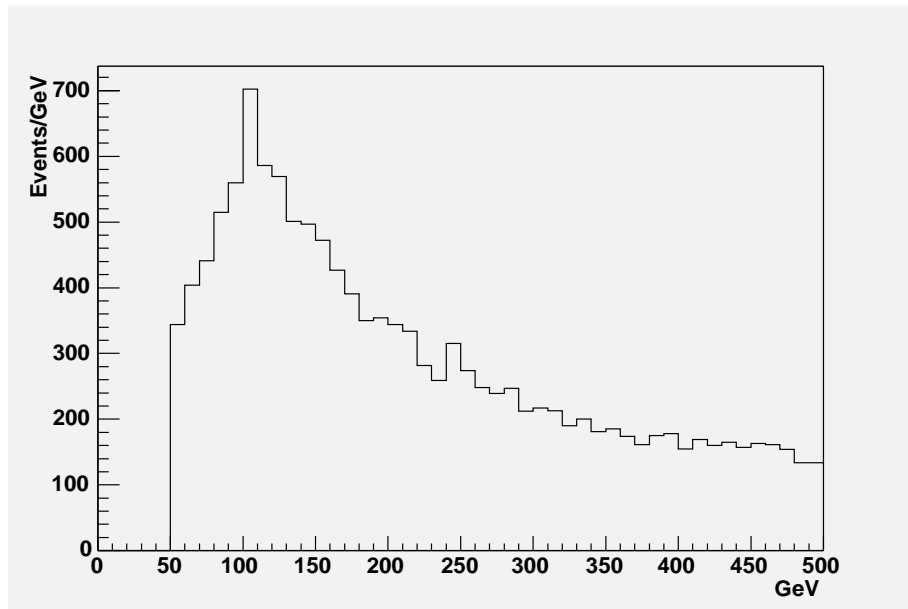


Figure 4: Transverse energy of leptons in BH events

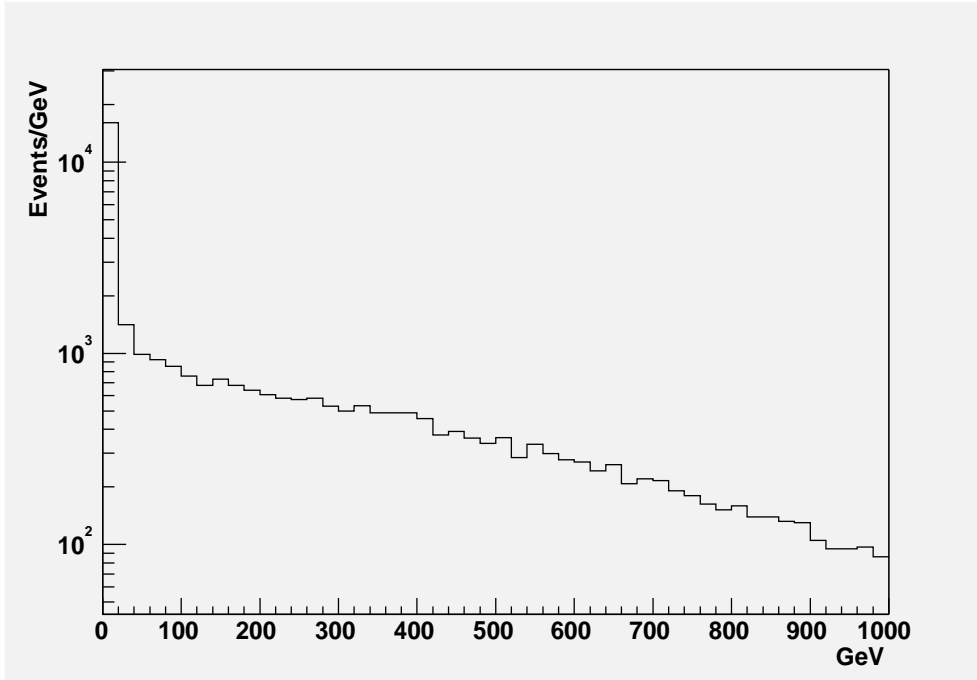


Figure 5: Missing transverse energy in BH events

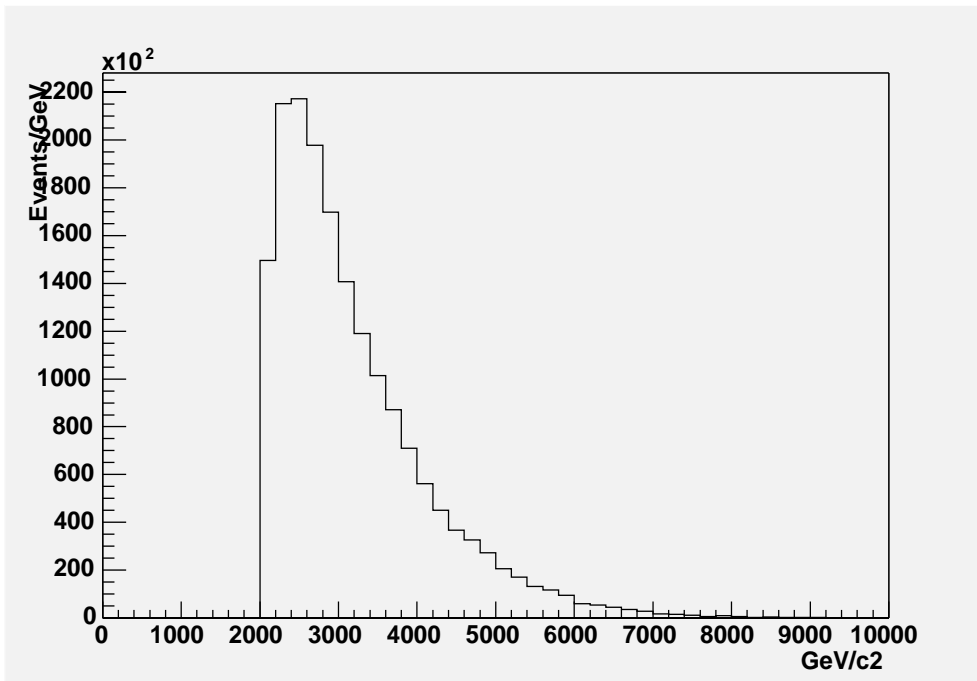


Figure 6: Black Hole mass

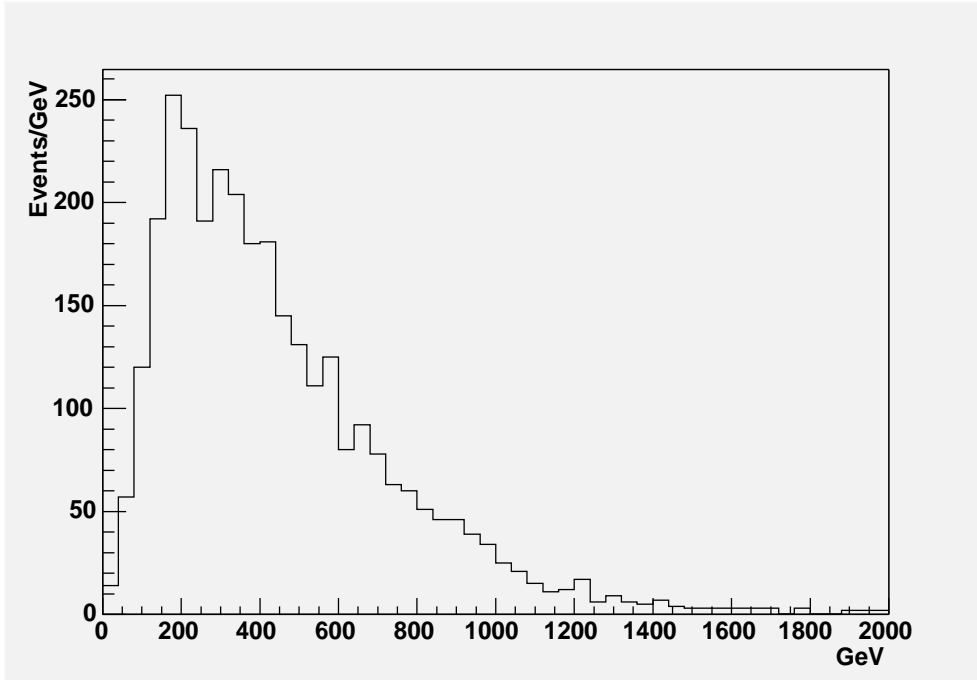


Figure 7: Transverse energy of the Higgs from BH decays

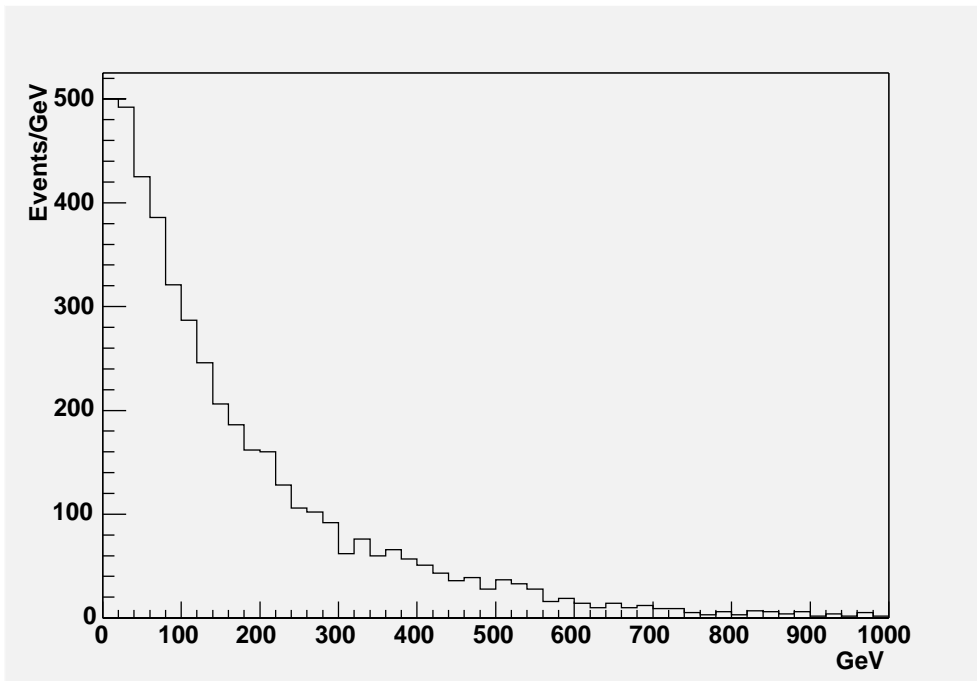


Figure 8: Transverse energy of  $b$  quarks from the decay of the Higgs boson

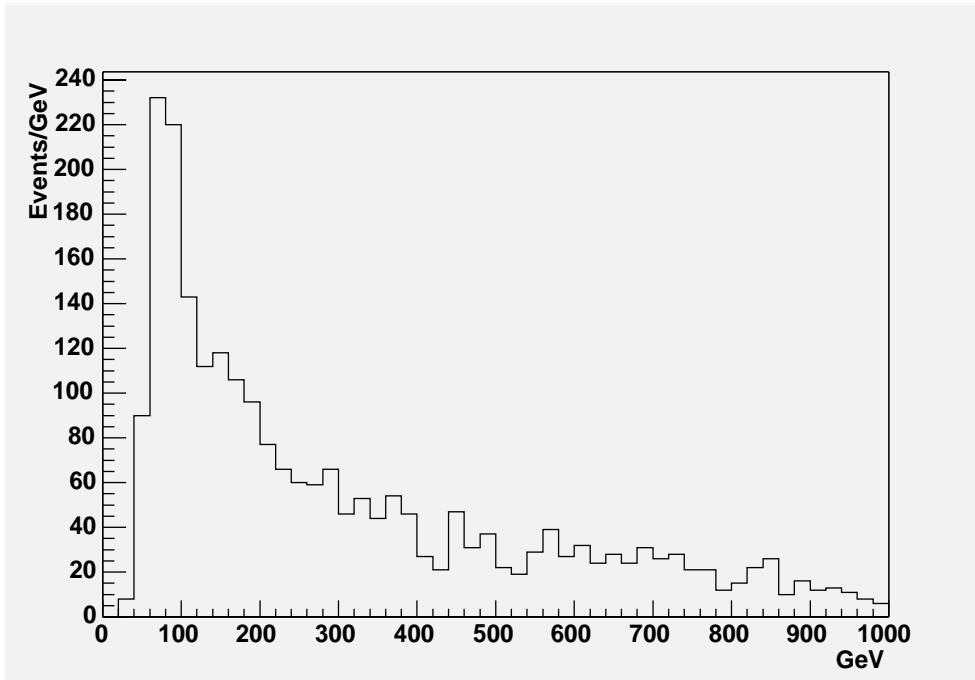


Figure 9: Transverse energy of jets for all di-jet combinations after cuts

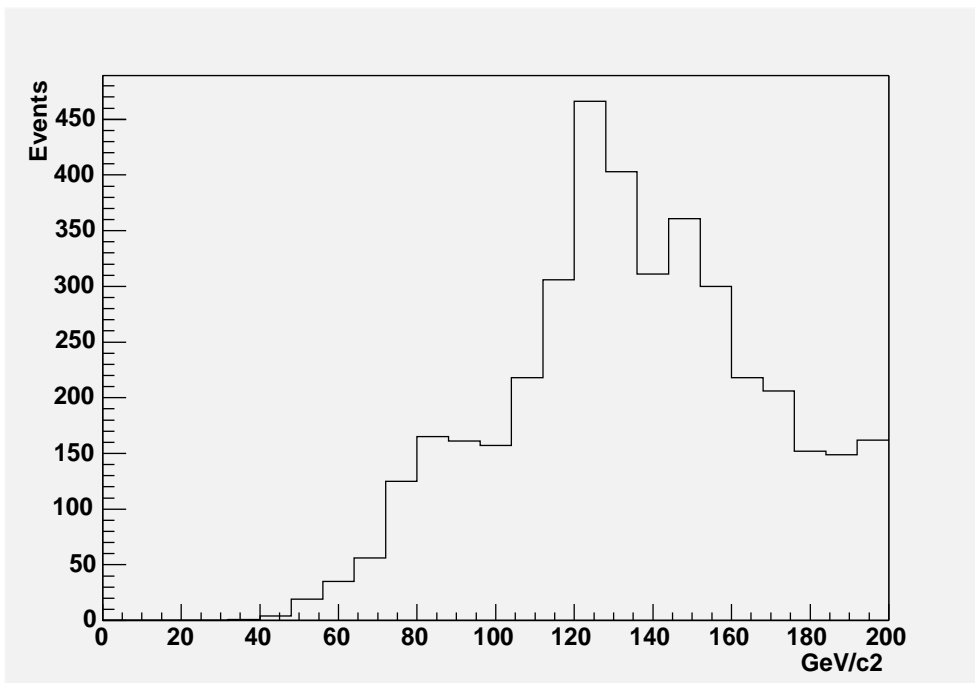


Figure 10: Di-jet mass spectrum at the generator level

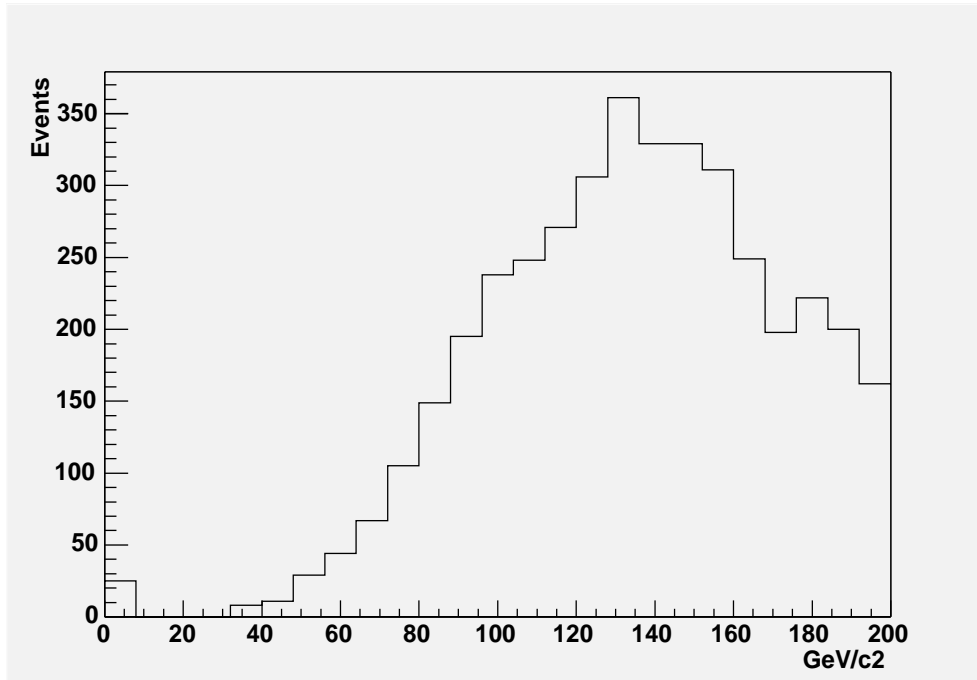


Figure 11: Di-jet mass spectrum after detector reconstruction

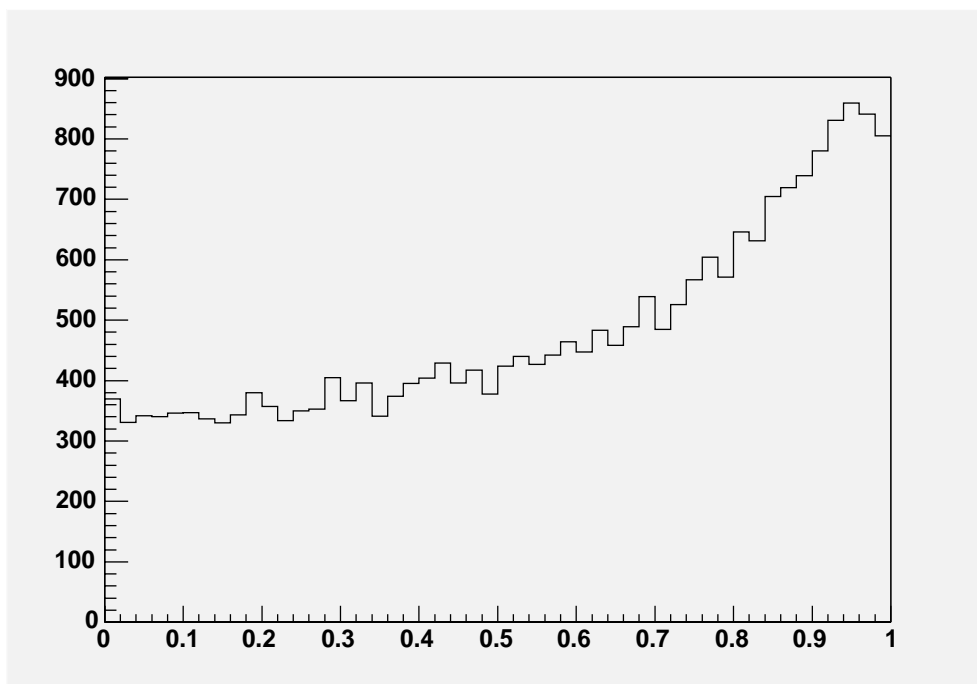


Figure 12: Distribution of  $\cos \theta^*$  for the di-jet system

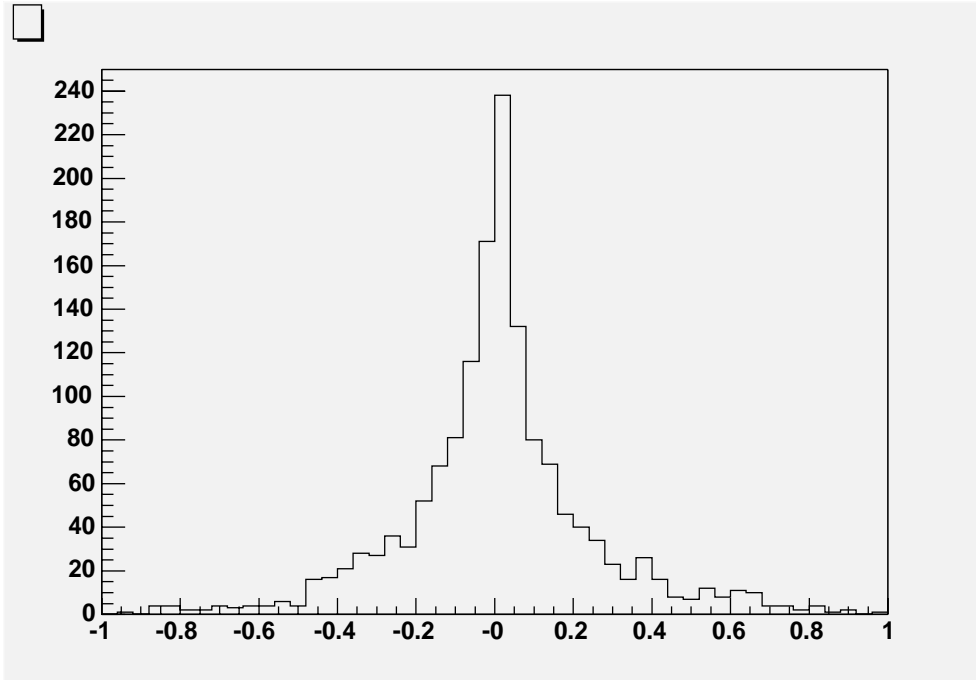


Figure 13: Distribution of  $\cos \hat{\theta}$  for  $b$  quark pairs from the Higgs decay

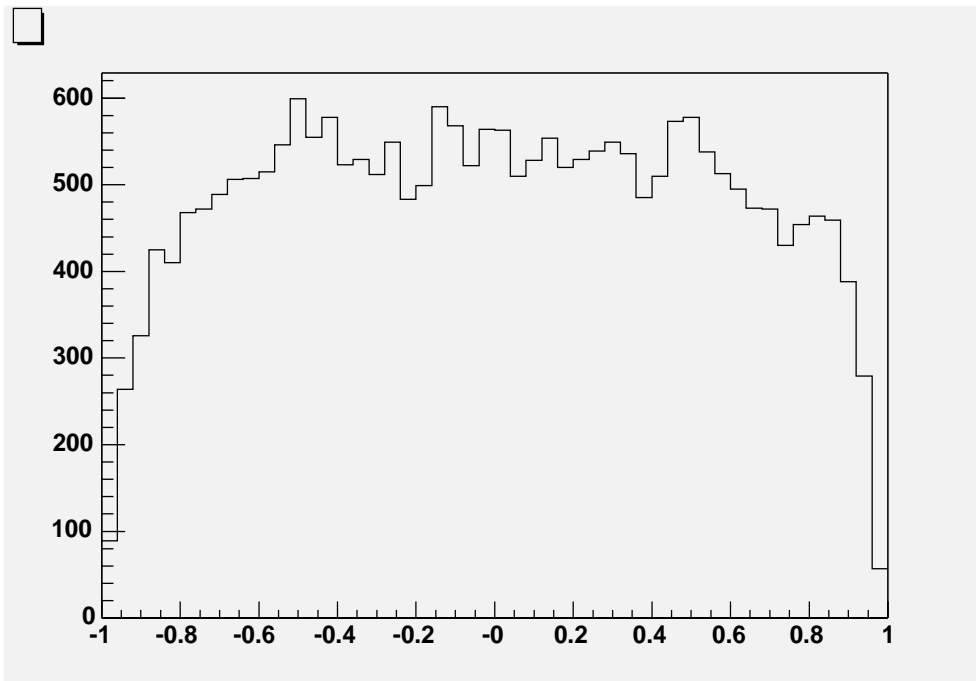


Figure 14: Distribution of  $\cos \hat{\theta}$  for all di-jet combinations



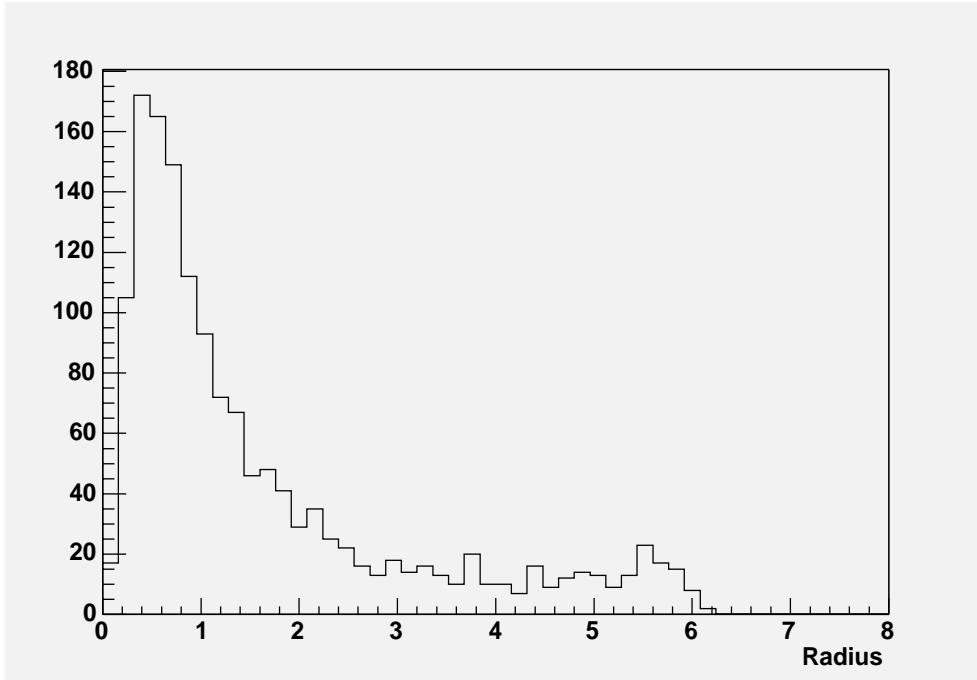


Figure 15: Distance in  $\eta$ - $\phi$  space between jet1 and jet2 from the decay of the Higgs

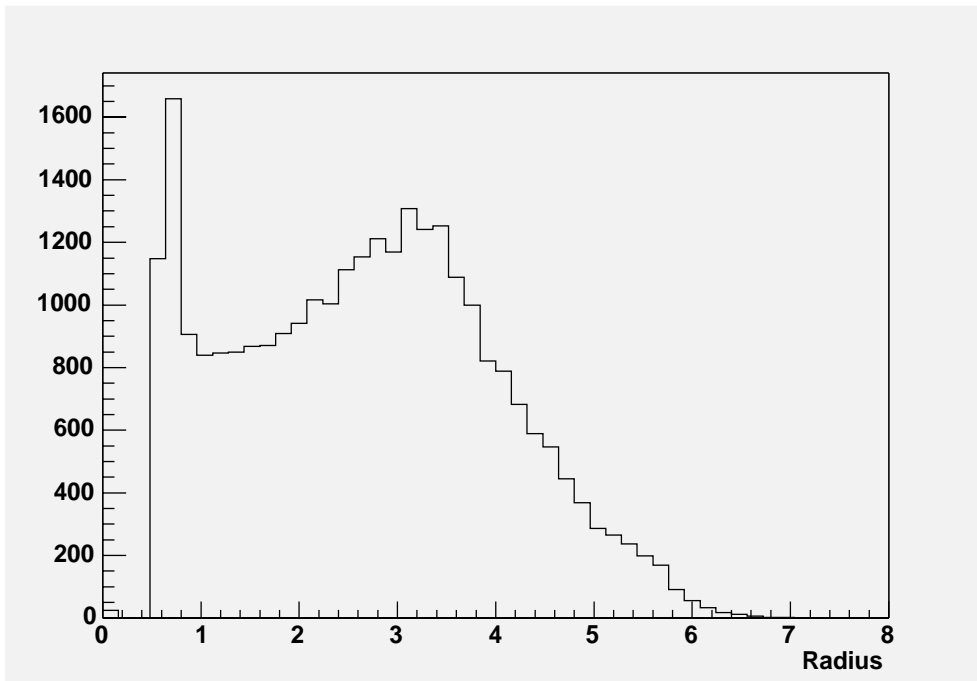


Figure 16: Distance in  $\eta$ - $\phi$  space between jet1 and jet2 for all di-jet combinations

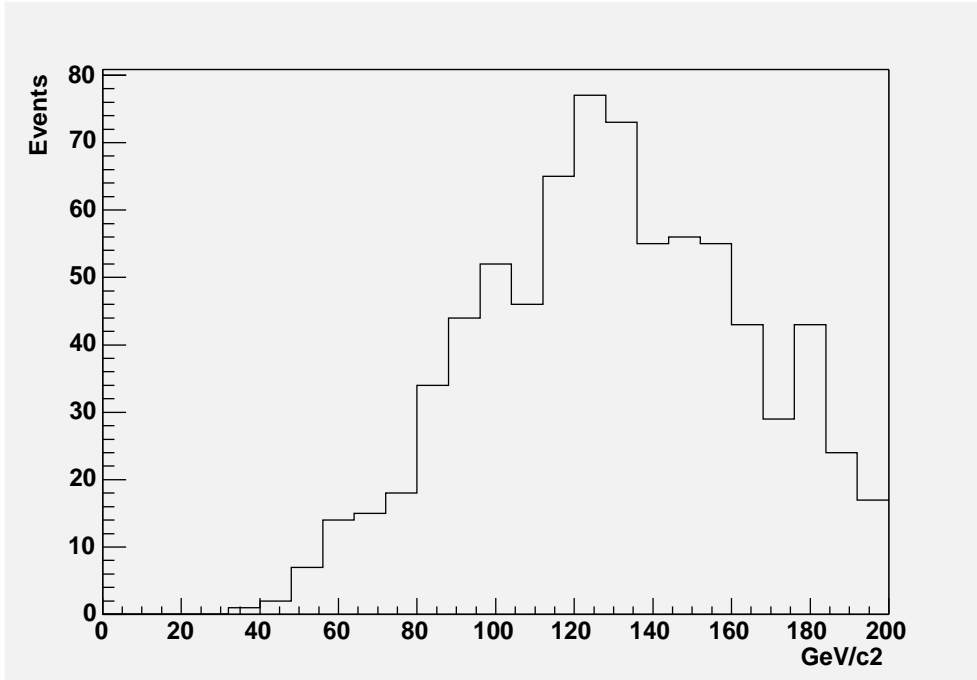


Figure 17: Di-jet mass spectrum for BH events after selection

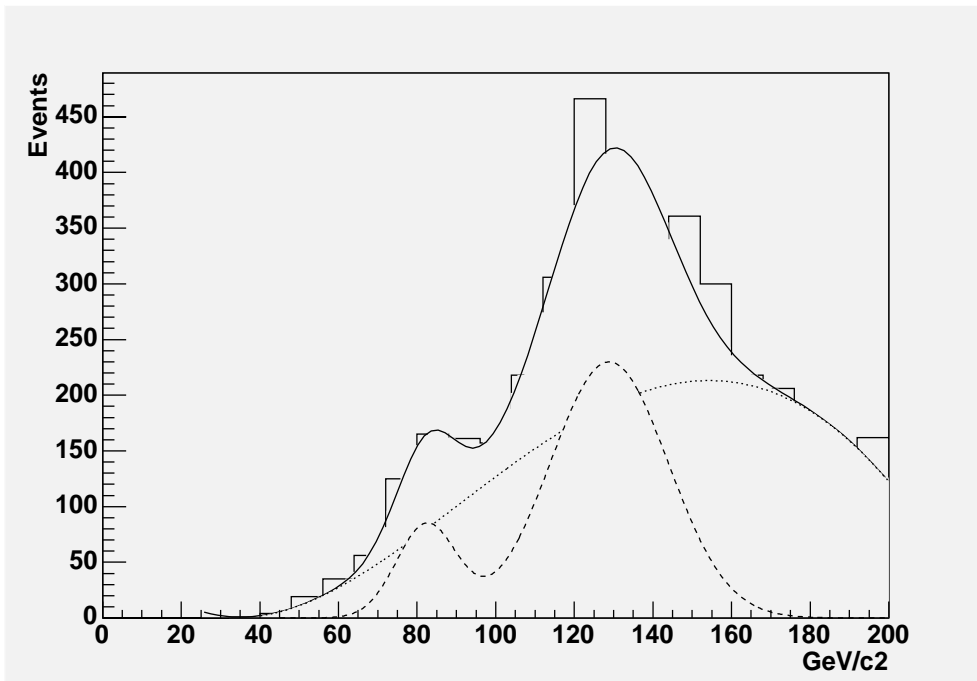


Figure 18: Di-jet mass spectrum and fits for particle clustering at the generator level

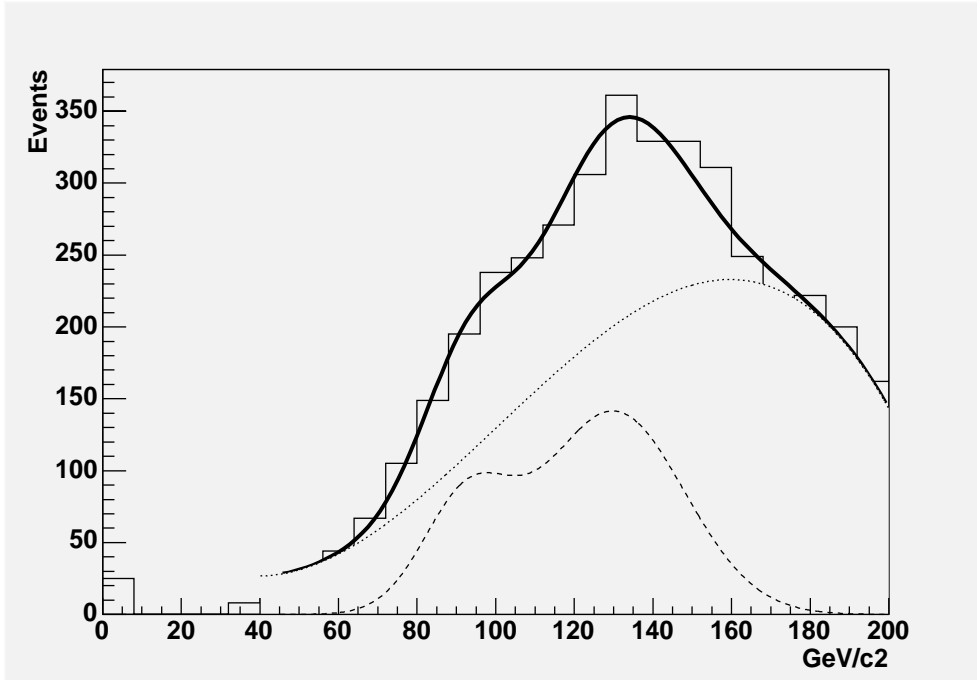


Figure 19: Di-jet mass spectrum and fits after reconstruction

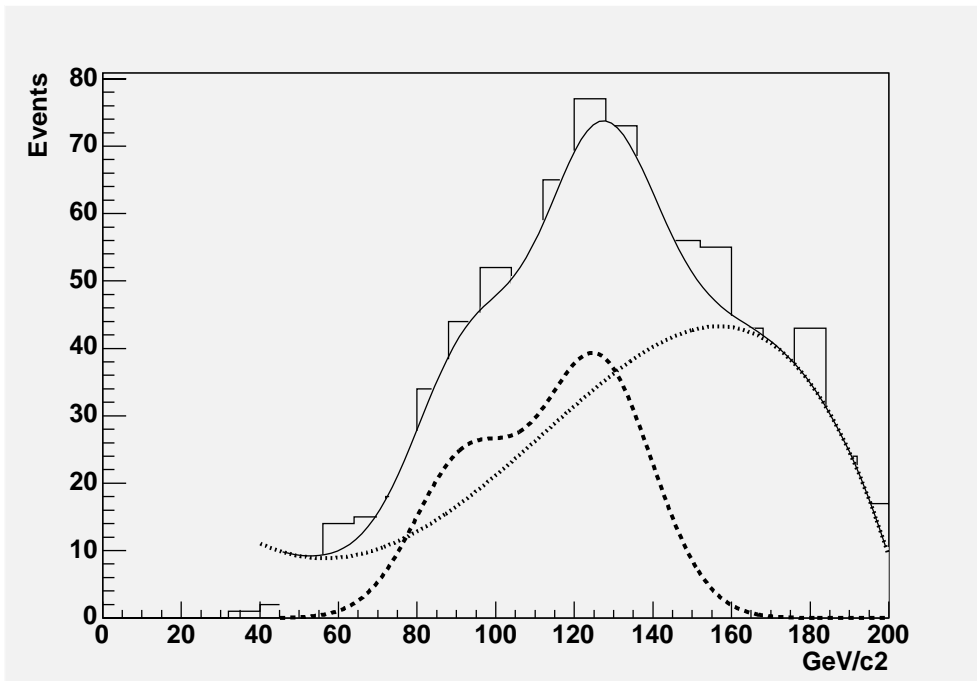


Figure 20: Di-jet mass spectrum and fits after selection

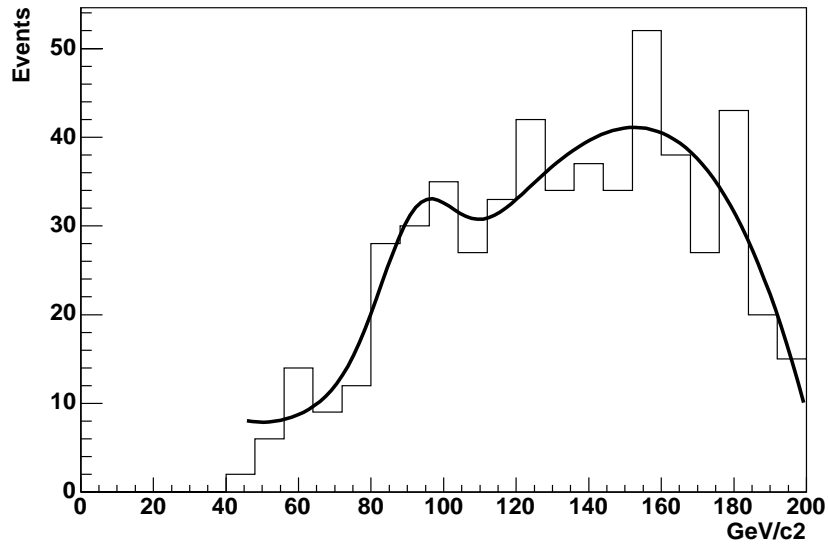


Figure 21: Di-jet mass spectrum and fits for BH events with no Higgs

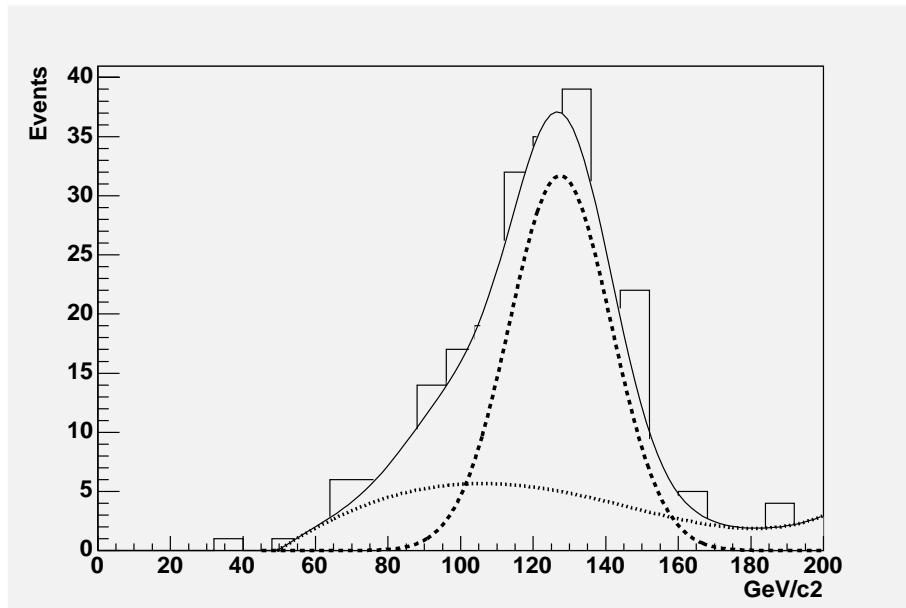


Figure 22: Di-jet mass spectrum and fits for BH events with at least one Higgs

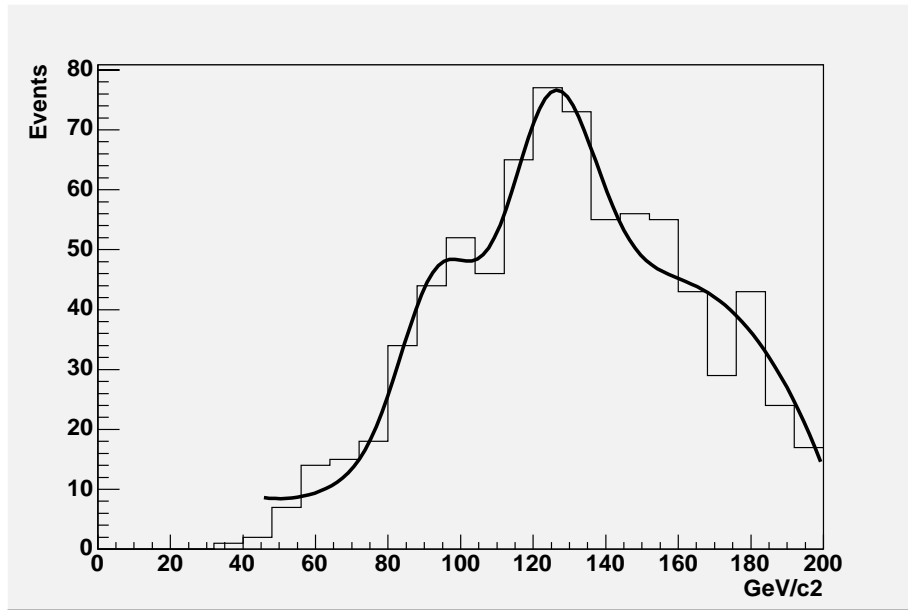


Figure 23: Spectrum and fit for all events constraining the shape of the background

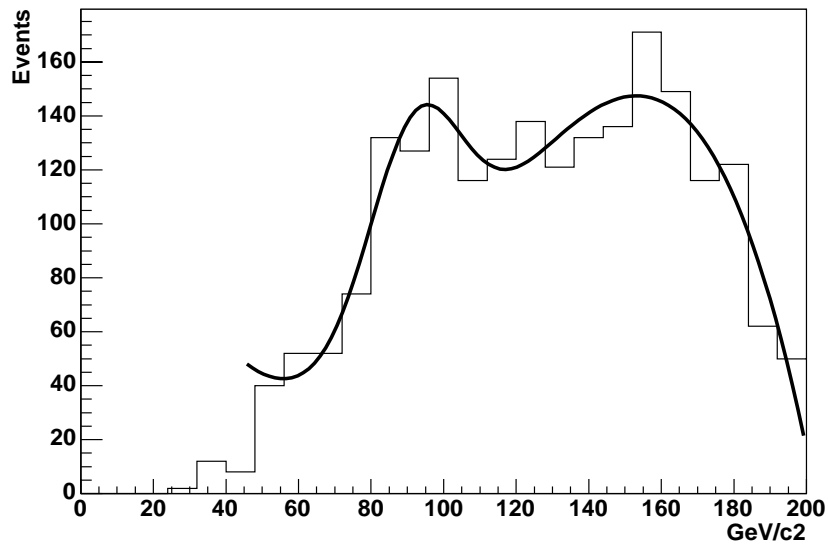


Figure 24: Di-jet mass spectrum and fits for BH events with no Higgs (no b-tag requirement)

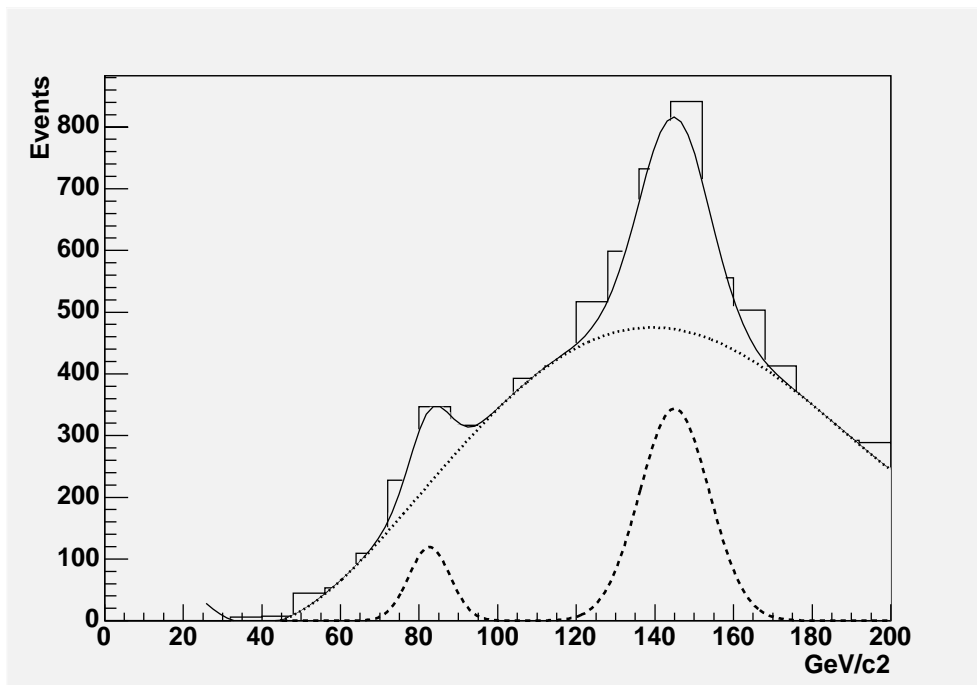


Figure 25: Di-jet mass spectrum and fits at the generator level for Higgs(150)